doi: 10.82124/CEAS-GNC-2026-006 CEAS-GNC-2026-006

Autonomous Aerial System for Deployment and Retrieval of Robotic Crawlers for Industrial Inspection

Jaime Ortuño-Conde Senior Robotics Engineer, CATEC, Seville, Spain.jortuno@catec.aero

Miguel A. Trujillo-Soto Head of Autonomous Systems Unit, CATEC, Seville, Spain.matrujillo@catec.aero

Antidio Viguria CTO of Avionics and Systems, CATEC, Seville, Spain.aviguria@catec.aero

ABSTRACT

Building upon the initial concepts for aerial robotic inspection introduced at ICUAS 2024, this paper presents the maturation and field validation of a fully integrated system for inspecting Corrosion Under Insulation (CUI) in petrochemical facilities. Developed within the EU-funded SIMAR project, the system features a fully actuated aerial platform with tilted rotors, specifically engineered for operation in complex, GNSS-denied environments. It is designed to flexibly integrate various inspection payloads and to perform safe take-off and landing maneuvers on intricate structures such as pipelines and robotic crawlers. The platform is further designed to maintain stable flight under wind gusts of up to 10 m/s and to remain operationally robust in the event of a single rotor failure.

The proposed work describes the complete autonomous workflow for the deployment and retrieval of a remote-operated inspection crawler equipped with industrial-grade sensors, including X-Ray (XR) and Pulsed Eddy Current (PEC), on active industrial pipelines. Key enabling technologies include a multi-sensor fusion algorithm for pipe detection and a vision-based strategy for precise crawler recovery.

The paper culminates with the results of a Technology Readiness Level 7 (TRL7) pilot demonstration carried out at an operational petrochemical facility operated by CHEVRON. During this validation, the SIMAR system demonstrated a 44-fold improvement in inspection efficiency compared to traditional manual methods, while completely eliminating human exposure to work at height.

Keywords: UAS, drones, control, tilted, fully-actuated

Nomenclature

Ψ, Θ, Φ	=	Euler angles (yaw, pitch, roll)
F	=	Force vector
F_x, F_y, F_z	=	Components of the Force vector
M_x, M_y, M_z	=	Components of the Moment vector
a	=	Acceleration $[m^2/s]$
m	=	Mass $[kg]$

g	=	Gravitational constant $[m/s^2]$
p, η	=	Position ($p = [x, y, z]^T$) [m] and Attitude ($\eta = [\phi, \theta, \psi]^T$) [rad] of the UAV
α_i, β_i	=	Tilt angles of rotor i [rad]
$F^{\max}\|_H$	=	Maximum lateral force in hovering [N] (components x, y)
$F_z^{\max}$	=	Maximum vertical force (thrust) [N]
D_x, D_y	=	Estimated aerodynamic drag [N]
T_i, Q_i	=	Thrust [N] and Torque [N·m] generated by rotor i
ω_i	=	Angular velocity of rotor i [rad/s]
$\vec{n}_i, \vec{r}_i$	=	Direction vector and position vector of rotor i
τ_i	=	Direction of rotation of rotor i
A	=	Control Allocation Matrix
KF	=	Kalman Filter
EKF	=	Extended Kalman Filter

1 Introduction

Inspection and monitoring of structural integrity in petrochemical plants, particularly corrosion under insulation (CUI) and the inspection of pipelines at height, are of critical importance for operational safety and cost efficiency. Traditional inspection methods for working at height involve scaffolding, rope access, and sometimes shutdown conditions that carry high risk, high cost, and extended times. In this context, robotic systems and, in particular, Unmanned Aerial Vehicles (UAVs) have emerged as transformative tools. UAVs enable access to difficult-to-reach zones, reduce human exposure, accelerate inspection procedures, and provide high-resolution data for advanced analysis. Recent studies demonstrate that UAV-based inspection methods significantly improve the efficiency and safety of petrochemical operations [1–4]. Furthermore, several reviews highlight how UAVs integrated with non-destructive testing (NDT) sensors, like pulsed eddy current (PEC) and ultrasonic, enable quantitative inspection of corrosion and material degradation [5, 6]. In petrochemical environments, where GNSS signals are often degraded by metallic structures and electromagnetic interference, robust navigation and localization solutions are required [7, 8]. This integration of UAV platforms, sensing payloads, and autonomy frameworks is increasingly recognized as a key for industrial plant inspection and maintenance.

A wide range of related work addresses UAV inspection of large-scale infrastructure. UAV-based vision systems have been applied to civil infrastructure inspection, leveraging 3D reconstruction and computer vision for defect detection [9]. In this context, frameworks like DRONIX demonstrate how automated trajectory planning and data capture with drones can be seamlessly integrated into construction pathology and infrastructure rehabilitation workflows [10]. Multi-UAV trajectory planning methods for complex structure inspection have been proposed to maximize coverage and efficiency in such inspections [11].

Moving towards contact-based inspection, aerial platforms such as the Voliro T combine omnidirectional flight capabilities—achieved through tilted rotors—with NDT tools to execute measurements on complex industrial structures without the need for scaffolding [12]. Beyond purely aerial platforms, recent approaches combine aerial and ground robots, creating hybrid UAV-crawler systems capable of performing contact-based NDT tasks in elevated and hazardous areas [5, 13]. For instance, air-ground hybrid systems like FalconScan allow a UAV to deploy and retrieve a specialized crawler to perform contact-based NDT inspections on elevated pipes, demonstrating feasibility even on small-diameter structures [14]. While these studies demonstrate the theoretical feasibility of advanced aerial and hybrid approaches, transitioning them from controlled laboratory settings to complex, real-world industrial environments remains a critical gap in the literature. Most existing solutions either rely on GNSS for navigation or struggle to maintain stability under realistic external disturbances.

Our previous work presented in ICUAS 2024 [8] introduced a novel UAV concept for metallic pipeline inspections. This article laid the foundation for landing on pipes (where we claimed the first system in the world able to land on pipelines in a real petrochemical facility), describing a platform with tilted rotors and the necessary perception algorithms for navigating without GNSS and for detecting pipelines. This concept was successfully demonstrated in the PILOTING project.

In summary, this paper presents the next step towards autonomous pipeline inspections by improving the previous system and resting on a solid foundation concerning UAV-based operations. The primary objective of this work is to present the maturation and field validation of a fully integrated, modular aerial robotic system capable of carrying different payloads for CUI inspection. To achieve this, several specific technical challenges had to be addressed explicitly: 1) ensuring stable flight and precise maneuverability in close proximity to complex metallic structures without GNSS, especially under wind disturbances; 2) developing robust, multi-sensor perception algorithms capable of reliable pipe and crawler detection; and 3) designing a mechanical coupling system that guarantees safe autonomous deployment and retrieval. Highlighting these technical constraints reveals the boundary conditions that must be considered for true industrial applicability.

The remainder of this paper is structured as follows: Section 2 details the modular robotic system design. Section 3 describes the autonomous stack, including the navigation, control, and perception modules. Section 4 presents the experimental setup, quantitative validation, and the limits of the proposed system. Finally, Section 5 draws the conclusions.

2 Robotic system design

The SIMAR robotic system is a comprehensive, fully integrated solution based on a modular architecture (see Fig. 1). It is fundamentally divided into two main components: the Ground segment and the Robotic segment. The Ground segment includes the Decision Making Tool (DMT), the Ground Control Station (GCS), the Augmented Reality (AR) interface, and the Artificial Intelligence (AI) module. The Robotic segment comprises the Unmanned Aerial Vehicle (UAV) and multiple easily interchangeable payloads, such as X-Ray (XR), Pulsed Eddy Current (PEC), and Visual modules. In a general operational workflow, these segments collaborate seamlessly: inspection missions are planned and managed via the DMT, executed autonomously by the UAV under the supervision of the GCS, and the acquired data is subsequently processed by the AI module to identify structural damages.

While the complete SIMAR architecture achieves this entire end-to-end data acquisition and processing pipeline, the scope of this paper is delimited to the Robotic segment technologies enabling the physical interaction with the infrastructure. Therefore, this work will focus exclusively on the object of study highlighted in the architecture: the Aerial Platform, the autonomous deployment and retrieval of the XR crawler, and the GCS acting as the primary User Interface (UI).

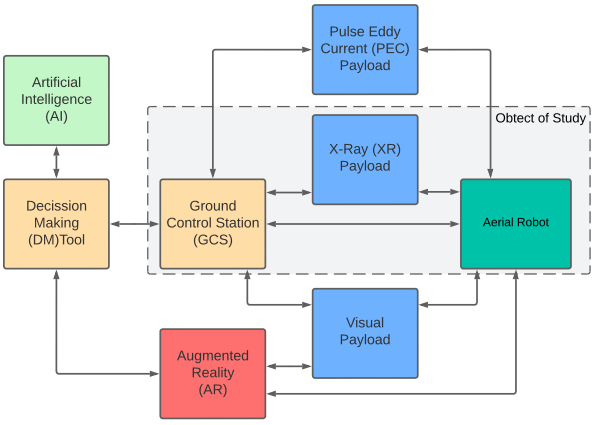

Fig. 1 General architecture of SIMAR system

2.1 Aerial Platform

The Aerial Platform developed consists of an octocopter designed with tilted rotors. This creates a fully actuated UAV able to generate horizontal forces allowing it to fly without changing its current

attitude. It was found in previous work [8] that this was a must for landing safely and with precision on cylindrical structures, in this case pipelines.

2.1.1 Design

This UAV was designed to meet strict operational requirements, including robustness against wind gusts (up to 10 m/s) and the ability to maintain flight in case of a single rotor failure. The design followed an iterative workflow of simulation, mock-up testing and full-scale integration.

Fig. 2 α and β angles for determining the rotors orientation

Rotor angles (α, β), shown in Fig.2, were optimized via a nonlinear programming problem in order to maximize lateral and vertical thrust efficiency while ensuring stability and rotor-failure compatibility.

The objective function:

$$f(\alpha_i, \beta_i) = (F_y^{max}|_H F_x^{max}|_H) \cdot \frac{F_z^{max}}{g} - abs(F_y^{max}|_H - F_x^{max}|_H)^3 \quad (1)$$

where $F_y^{max}|_H, F_x^{max}|_H$ are the maximum lateral forces during hover, F_z^{max} is the maximum vertical lift, and g is the gravity constant, is formulated to minimize the absolute difference between the horizontal and vertical thrust capabilities, ensuring a balanced control authority, while simultaneously penalizing configurations that significantly reduce the maximum vertical lift. Constraints ensured sufficient control authority against aerodynamic drag (D_x, D_y) and adequate torque for roll, pitch, and yaw.

In order to validate the results, three preliminary designs were tested with different configurations of rotor dispositions. The best approach found was a platform with all rotors tilted, that presented good yaw capabilities while reducing interaction between overlapped rotors, good flight performance in general and showcasing the ability to counteract winds of around 10 m/s using only lateral forces.

Fig. 3 Final UAV, 2nd version rotors disposition

The full-scale UAV (Fig.3) was built following the previous mentioned configuration optimizing the structural design by a selective use of carbon fiber. The arms were delimited by a central rotation piece and a clamp placed at the outer part of the frame for allowing UAV reconfiguration. The sensor suite selected for the UAV is composed of a 3D LiDAR and IMU for navigation, two 2D LiDAR and a depth camera for pipe detection, and, finally, a camera pointing down for crawler recognition.

2.2 Coupling mechanism

Modularity is a main feature of SIMAR project. This aircraft acts as a "mothership" able to transport and operate different interchangeable payloads.

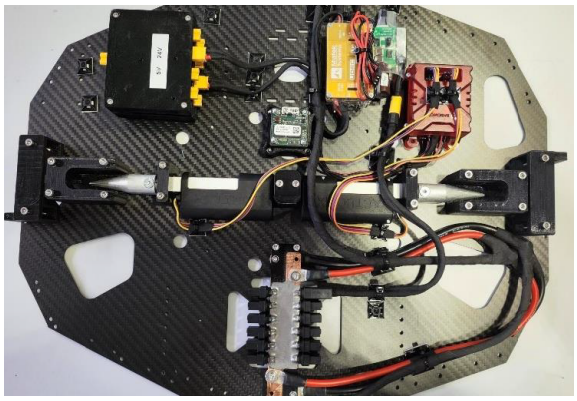

Fig. 4 Active system of the coupling mechanism onboard

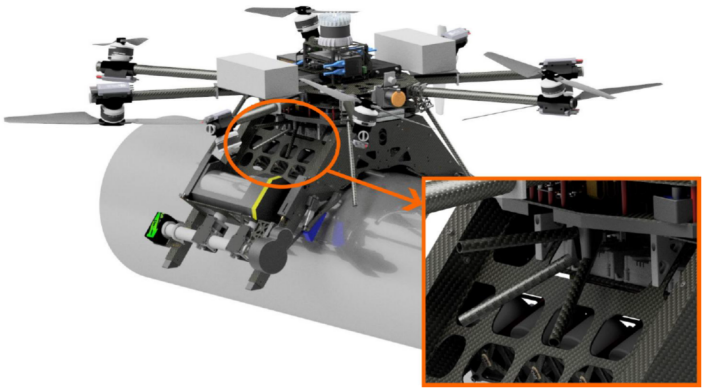

Fig. 5 Final UAV, guiding mechanism between UAV and XR crawler

This integration is physically made through a mechanical device custom made for SIMAR that can attach and detach any of the payloads in less than 1 minute composed of the following components:

- Active Mechanism (on UAV): Placed at the base of the UAV (Fig.4), this mechanism uses two linear actuators that move a conical plug. These conical plugs have to be inserted through the passive mechanism located in the crawler locking and ensuring a safe coupling process.
- Passive Mechanism (on Payloads): Placed on top of the payloads, has two metallic rings. These rings guide the conical part from the active mechanism for ensuring a robust lock while coupling.

In addition to this, there is another mechanical part playing an important role while coupling for retrieving the crawler. This is the guiding mechanism (Fig.5), two "V-shaped" structures located at the bottom of the UAV that guides the UAV while landing on top of the crawler. This system allows for lower precision while landing ensuring the successful attachment of the UAV and payload.

2.3 XR crawler

The payload system presented in this paper will only be the X-Ray one. This is a robotic crawler remote-operated with 13 Kg weight, designed specifically for moving along the top surface of pipelines. Its main function is to deploy an X-Ray generator and X-Ray detector placing it facing the bottom part of the pipe (at 6 o'clock position) for taking images of that part where the CUI is most likely to appear.

The design of the final crawler (shown in Fig.6) is the result of an iterative process prioritizing the low weight, robustness and operational simplicity. The movement system is composed of two sets of 3 motorized wheels with encoders plus 2 free wheels guaranteeing enough friction on top of the insulated pipelines. It incorporates a clamping system that holds the crawler in place adding extra support while deploying or retrieving the crawler. The X-Ray deploying mechanism guarantees the X-Ray generator and detector are placed down to the bottom of the pipe where 2 servo motors control the movement from the storage to the deployed position.

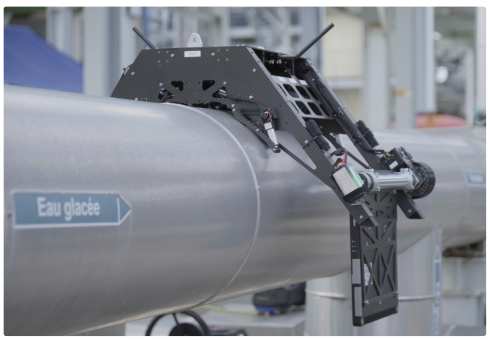

Fig. 6 Crawler XR on top of a pipeline while performing X-Ray inspection

2.4 GCS

The GCS is the central hub of the robotic systems. It is the human-robot interface acting as a control center and data management. The GCS is built using a modular system based on RViz (ROS 3D visualizer) [15]. This choice allows a 3D real time visualization, telemetry from the Aerial Platform and the payloads at the same time as sending control commands to these payloads. Being built in RViz gives the required modularity having implemented a different plugin for different systems:

- Plugin for UAV (see Fig.7): Monitors the UAV state, displays the FPV camera, and allows an operator to control the UAV sending high level commands.
- Decision Making Tool (DMT) plugin: Manages the download of inspection missions and the upload of results.
- Payload plugin (XR, PEC, Visual): Each payload has its own plugin that offers specific control interfaces for each payload allowing the data acquisition and the remote operation.
- Run Data Gather plugin: standardizes the data collection and metadata for all inspection types providing a results data pack with the required format.

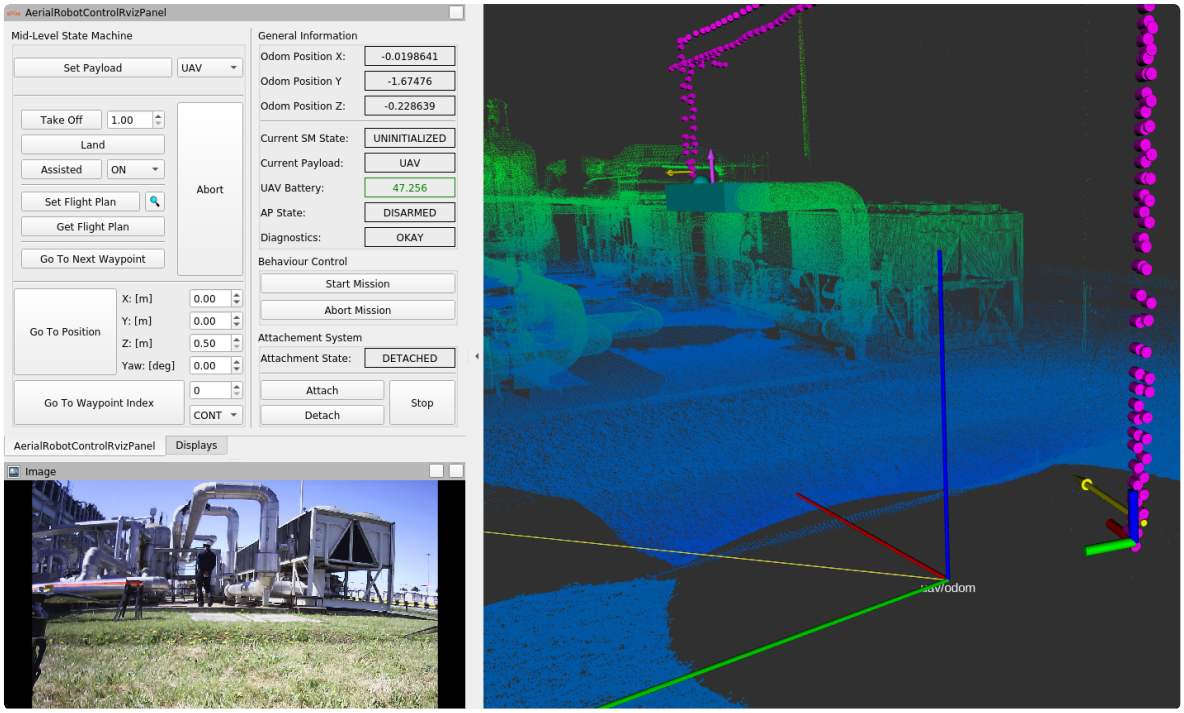

Fig. 7 UAV plugin for GCS. UAV landed after XR deployed on pipeline

3 UAV Autonomous Stack

In order to operate in a complex and cluttered environment like a petrochemical facility where GNSS has poor signal, the system must present a robust architecture for guidance, navigation, and control. This paper presents an autonomous stack (see Fig. 8) where the mission is handled by a behavior tree receiving as inputs information from the perception and navigation modules. This information is used to generate the guidance transmitted to the controller, which ensures the UAV performs the requested commands in stable flight.

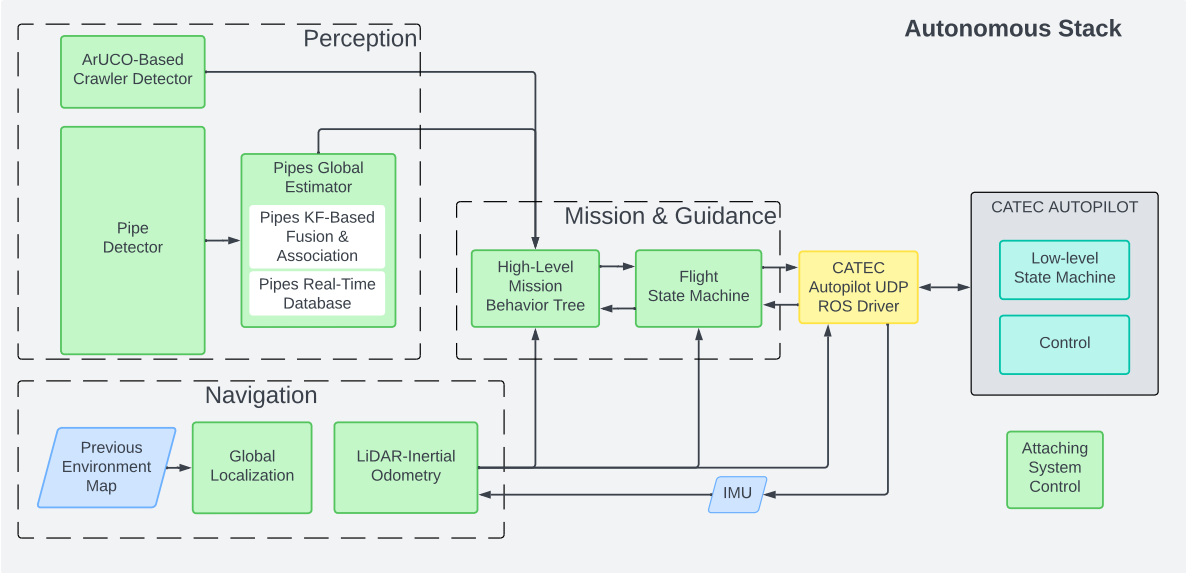

Fig. 8 UAV autonomous stack diagram. Key acronyms include Kalman Filter (KF), Robot Operating System (ROS), User Datagram Protocol (UDP), and Inertial Measurement Unit (IMU).

3.1 Navigation

The system's navigation, designed for GNSS-denied environments, is a critical component for autonomous operations. The navigation module, consists of a LiDAR-Inertial odometry and a global localization (see Fig.9).

- The Global Localization Module, based on the algorithm DLL (Direct LiDAR Localization) [16] is a point cloud matcher. Provided with a previously generated map of the environment and the current seen point cloud, it corrects the offset between the relative reference frame and the global reference frame at a low frequency.
- The LiDAR-inertial Odometry is an algorithm based on LIO-SAM [17] that fuses data from 3D LiDAR and IMU (Inertial Measurement Unit). It provides the position and attitude of the UAV at high frequency and with high precision in the relative reference frame, allowing a stable control and the execution of autonomous missions.

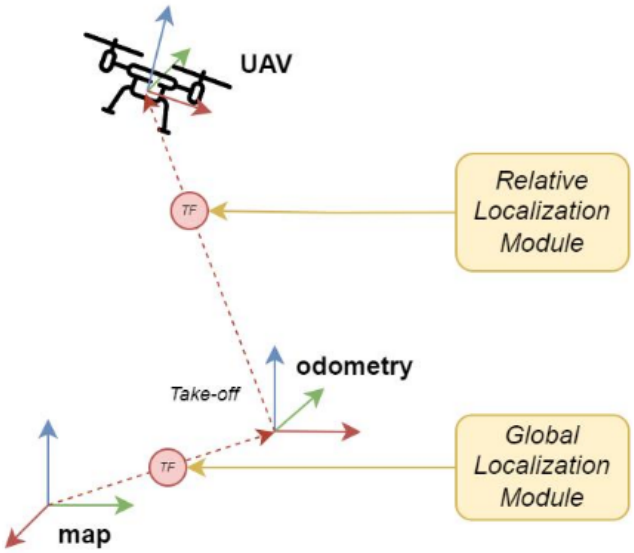

Fig. 9 Reference frames of the Navigation

3.2 Control

The UAV's control system is developed on a custom autopilot developed by CATEC. The tilted rotors configuration is one of the keys because it allows to separate the translation from the attitude control meaning the UAV can generate horizontal forces for moving horizontally while maintaining the attitude fixed, in this case roll and pitch to zero.

3.2.1 Control Architecture

The control architecture shown in Fig.10 is divided in three different main blocks executed in cascade:

- Attitude Control (Orange block of Fig.10): Implements a Proportional Derivative Integral (PID) cascade controller that stabilizes the UAV in roll, pitch and yaw (ϕ, θ, ψ). When flying using the "lateral forces fly mode", this controller keeps roll and pitch to zero ensuring the platform flies level while moving horizontally.
- Lateral Forces Control (Purple block of Fig.10): also implements a cascade PID controller converting the velocity reference (x, y, v_x, v_y) into a desired lateral force vector (F_x, F_y).
- Z Control (Blue block of Fig.10): an independent PID cascade controller that manages the altitude and the vertical velocity (z, v_z)

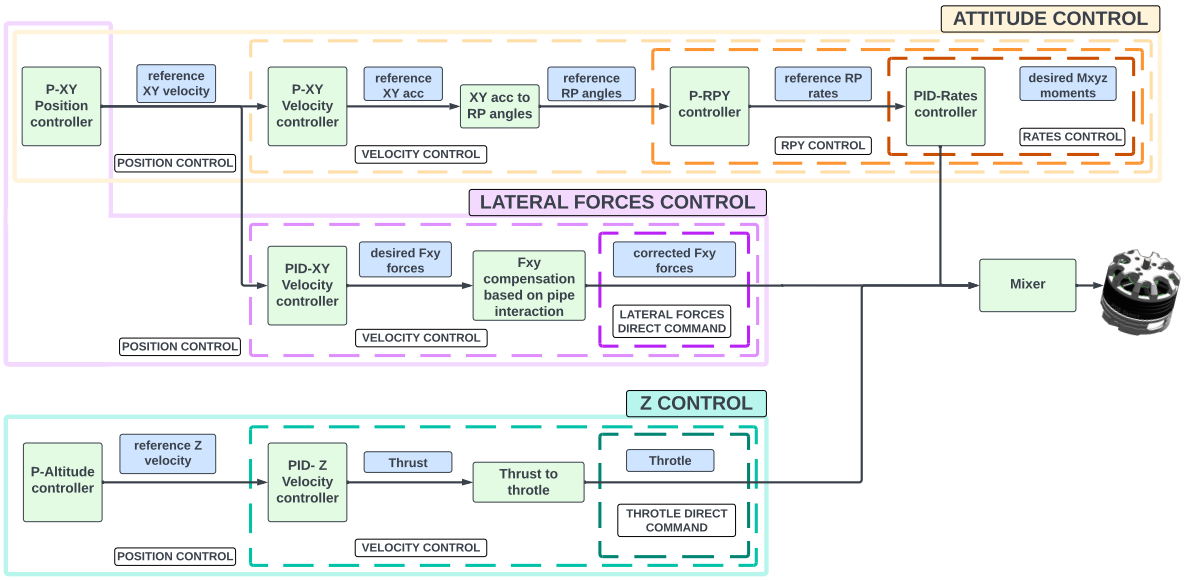

Fig. 10 UAV control architecture

3.2.2 Mixing Strategy

The mixer is a software component converting the output of the three different controllers (F_x, F_y, F_z, M_x, M_y, M_z) into the individual Pulse Width Modulation (PWM) for each of the 8 rotors where the forces/momentum generated (F_i, M_i) and the velocity of the rotors (ω_i) are defined by the dynamical model of the rigid solid:

$$\begin{bmatrix} F_x \\ F_y \\ F_z \end{bmatrix} - m\vec{g} = \sum_{i=1}^{n} T_i \cdot \vec{n}_i$$

$$\begin{bmatrix} M_x \\ M_y \\ M_z \end{bmatrix} = \sum_{i=1}^{n} (Q_i \cdot \vec{n}_i \cdot \tau_i + \vec{r}_i \times (T_i \cdot \vec{n}_i))$$

where T_i and Q_i are the thrust and torque of the rotor i, $\vec{n}_i$ and $\vec{r}_i$ are the direction and position vectors, and τ_i indicates the direction of rotation of the i-th rotor. Expanding the equations and grouping terms,

the following expression can be written:

$$\begin{bmatrix} F_x \\ F_y \\ F_z \\ M_x \\ M_y \\ M_z \end{bmatrix} = A_{6\,\mathrm{x}\,n} \cdot \begin{bmatrix} \omega_1^2 \\ \vdots \\ \omega_n^2 \end{bmatrix}$$

Given the system has 8 actuators for 6 DoF (Degrees of Freedom), the control set will not be unique for a set of forces and moments. The control solution is being computed using the Moore-Penrose pseudo-inverse since, based on this approach, the control set achieved is the one with minimum Euclidean norm that guarantees the most efficient alternative in terms of energy.

In addition, a mixed attitude-forces control has been designed to allow, if necessary, the combination of lateral forces and attitude commands to achieve greater lateral force and thus, better response to intense wind gusts.

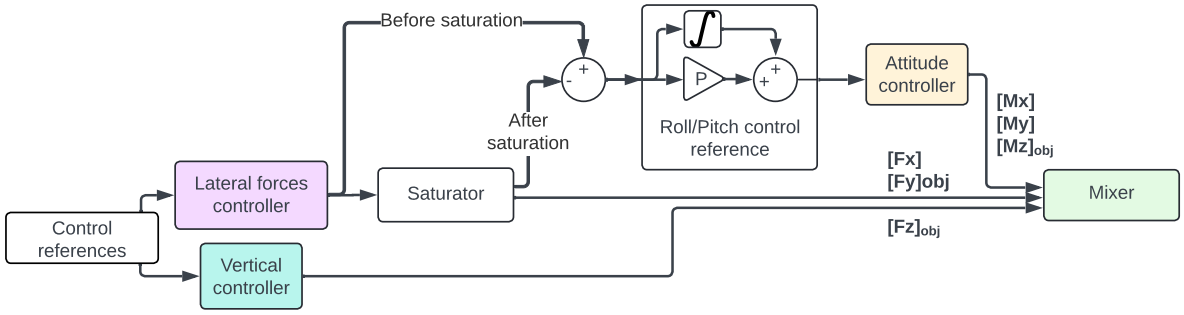

Fig. 11 Mixed Attitude Forces control

The approach, presented in Fig.11, relies on detecting a control command in lateral forces that surpasses the physical threshold of the platform. In such cases, the portion of this command that cannot be fulfilled solely by lateral forces is converted to a reference for roll or pitch.

Finally, there is a reactive control for mitigating rollover caused by pipe contacts. The approach for landing on the pipe and on the crawlers represents the most critical phase of the operation. In particular, the contact between the UAV and the pipe or crawler can create rollover moments compromising the aircraft. The logic is such that if, during an approach and landing on the pipe or crawler, a deviation in roll that exceeds a threshold occurs, a control action is executed to alleviate the contact.

3.3 Perception

The autonomous stack shown in Fig.8 contains a perception module composed of two main components: The "Pipe Detector" [8] and the "ArUCO Crawler Detector" [18] [19]. These are the input for the guidance system in order to land on pipelines and on the crawlers. Detections from both modules are transformed to the global reference frame given by the Navigation module.

3.3.1 Pipe detection module

The autonomous stack shown in Fig. 8 contains a perception module composed of two main components: The "Pipe Detector" [8] and the "ArUCO Crawler Detector" [18] [19]. These are the input for the guidance system in order to land on pipelines and on the crawlers. Detections from both modules are transformed to the global reference frame given by the Navigation module.

In order to be able to land autonomously on pipelines, the guidance system requires a position estimation of the pipe. This feature is provided by the Pipe Detection Module. The module architecture, shown in Fig. 12, is based on sensor fusion for a better estimation [20]. The system uses a depth camera and two 2D LiDAR. These sensors are processed by two independent detectors: "Cloud Pipe Detector" and "Laser Pipe Detector".

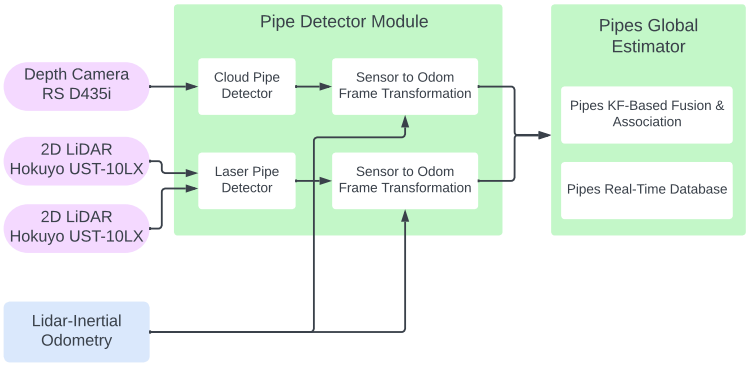

Fig. 12 Pipe detector architecture

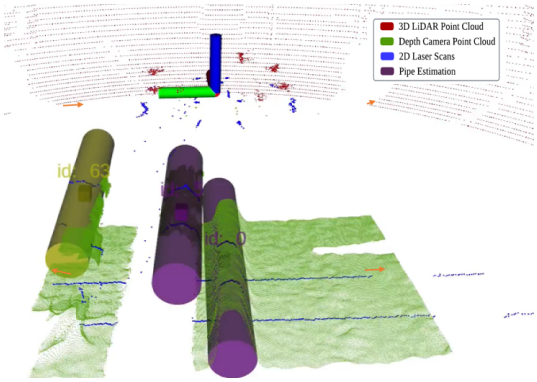

Fig. 13 Test of Pipe Detection

The detections from both modules are transformed to the global reference system. Next, the "Pipes Global Estimator" fuses these detections with a Kalman Filter. Pipe detections are stored in a database that updates its position and radius with new detections. The final result is a stable pipe estimate that serves as a reference for the guidance system. As detailed in a specific evaluation of this perception architecture [20], this fused tracking system yields a mean geometric distance error of 2.6 to 2.9 cm and an angular deviation between 1.43° and 3.2°, ensuring the precision required for a safe touchdown.

A detection example is shown in Fig. 13 where the pipe detector was able to detect different pipes where purple represents the current estimate pipes and yellow the previously estimated ones.

3.3.2 Crawler detection module

For the crawler recovery phase, the guidance system must identify with precision the 3D pose of the crawler, which is located on top of a pipeline. This task is performed using the "Crawler Detection Module" (Fig.14).

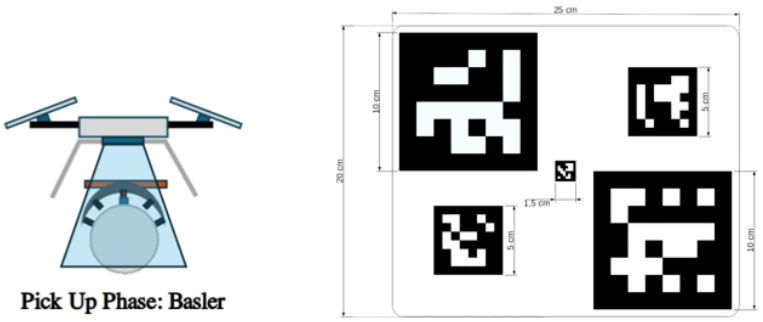

Fig. 14 Crawler detector representation

The system is based on computer vision using a camera mounted at the bottom of the UAV and facing down. These cameras must identify a set of 5 ArUCO markers with different sizes located on top of the crawler. The use of different sizes ensures a higher range of detection and guarantees pose estimation even if there is some marker out of the image frame or presenting occlusion. Once the markers are detected, the system fuses these detections with a Kalman Filter providing a single 3D pose estimation of the crawler target.

3.4 Mission Control and Guidance

The mission and Guidance is developed with a two layers architecture for ensuring safety and robustness:

- Flight State Machine: Manages the safety regarding the flying actions in autonomous. It is a bridge for sending commands to the autopilot.
- High-Level Behavior tree: Handles the mission logic specifying the tasks for the autonomous system. This also acts as the guidance module for the UAV.

3.4.1 Flight State Machine

This is an important component acting as a bridge between the high level decisions and the autopilot. This module guarantees that the autonomous flight actions are executed safely. It manages the transitions between fly modes and commands basic actions to the autopilot.

The State Machine, shown in Fig.15 differentiates the mission from manual (green states) to autonomous, defines stationary states (blue) for the autonomous behavior such as "LANDED" and "HOVERING" , handles action states (yellow) such as "TAKINGOFF", "LANDING" and "GOING_TO".

Additionally, it has a fail-safe layer added to it. In case of failure is detected, this gets triggered and the system goes to an emergency state (red) as "WAITING", "EMERGENCY_RTH", "EMERGENCY_LANDING", "EMERGENCY_LANDED" depending on the level of the failure.

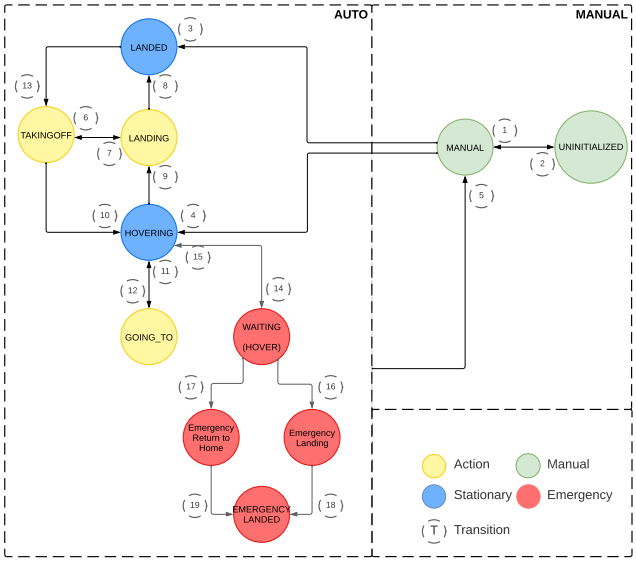

Fig. 15 Flight state machine architecture

3.4.2 High-Level Behavior Tree

The high-level Behavior Tree (BT) is the brain of the mission. It implements the logic for the required task following a sequence of actions in order to reach an objective. For the objective of this paper, there are two missions developed with BT: "Deploy XR crawler" and "Recover XR crawler".

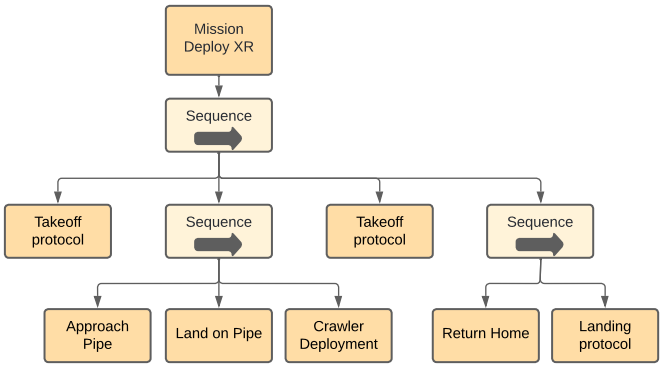

Fig. 16 Simplified Behavior Tree for XR deployment

In general, the execution of a mission is done in a sequence mode that executes other sub-trees, for example (see Fig.16):

- Takeoff protocol: BT calls the takeoff action from the Flight State Machine (Fig.15) and waits for the state to change from "LANDED" to "HOVERING" passing by "TAKINGOFF".
- Main sequence: this is the sequence where the task is going to be performed. In this case the UAV will have to "Approach the pipe", "Land on the pipe" and finally "Deploy the crawler" by releasing

the coupling mechanism. In this sequence, the BT acts as a guidance system receiving information of the UAV from the Navigation module, the target pose is provided by the Perception modules and commands the UAV in order to reach the target by using of the "Flight State Machine".
- Final sequence: Once the crawler has been deployed and the UAV is back "HOVERING", the system is ready to go back to the "home" position. Again the BT guides the UAV to "home".
- Landing Protocol: BT calls the landing action from the Flight State Machine from 15 and waits for the state to change from "HOVERING" to "LANDED" passing by "LANDING".

This structure ensures the maximum safety against any failure or abort during any part of the mission. It has been proven to be very robust and flexible adding modularity to the whole system.

4 Demonstration and Validation

The SIMAR system was demonstrated and validated in a final pilot demonstration at Chevron's Oronite petrochemical facility in Gonfreville, France. The scenario for the test was a water treatment unit with active pipes with diameters from 4 to 10 inches located at different heights. During the demonstration, the system successfully executed the autonomous mission workflow point to point (deployment, inspection, recovery). This demonstrated the real capabilities of the system in real industrial environments, including flying with wind gusts of up to 8 m/s.

4.1 Autonomous mission execution

The complete cycle of execution was performed as follows:

- Deployment of the XR crawler: The UAV, carrying the XR crawler, flew nearby the target pipe to be inspected. Then, using the information from the Pipe Detector, the UAV landed softly on top and deployed the XR crawler. Finally it took off from the crawler and performed a "Return to home" maneuver. Fig.17, 1 shows the UAV landing on the pipe while Fig.17, 2 shows the UAV landed on the pipe.
- Inspection phase: The XR crawler was remotely operated by an inspector from the GCS moving along the pipe for inspection purposes.
- Recovery of XR crawler: The recovery process, the most critical autonomous task, is shown in Fig.18. Image labeled 1 illustrates the moment when the UAV is descending on top of the crawler, 2 shows the last phase of landing on the crawler, in 3 the UAV is already landed and attaching the XR crawler using the coupling mechanism. Finally, 4 shows the UAV taking off from the pipe carrying the XR crawler. The mission ends with the UAV landing successfully in the home position.

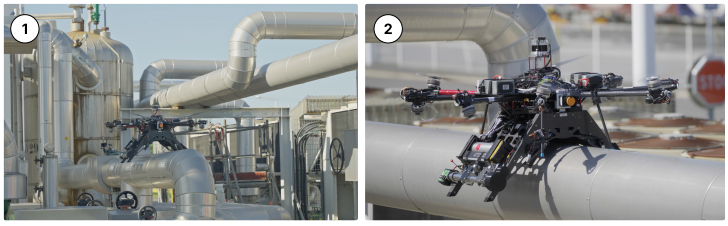

Fig. 17 Deployment mission during the final validation

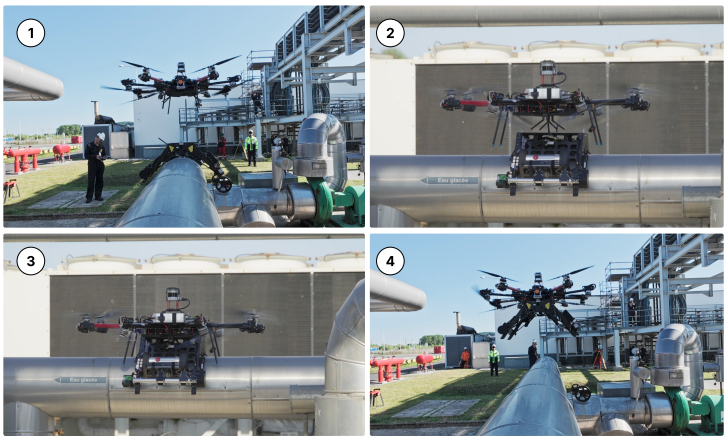

Fig. 18 Recovery mission during the final validation

4.2 Perception validation

The autonomous operation was possible thanks to the performance of the perception in the real environment. For landing on the pipe, the pipe detector worked perfectly during the landing process. Fig.19 shows the detected target pipe (purple) and the GCS at the same moment where it is possible to see the UAV placed on top of the target pipe.

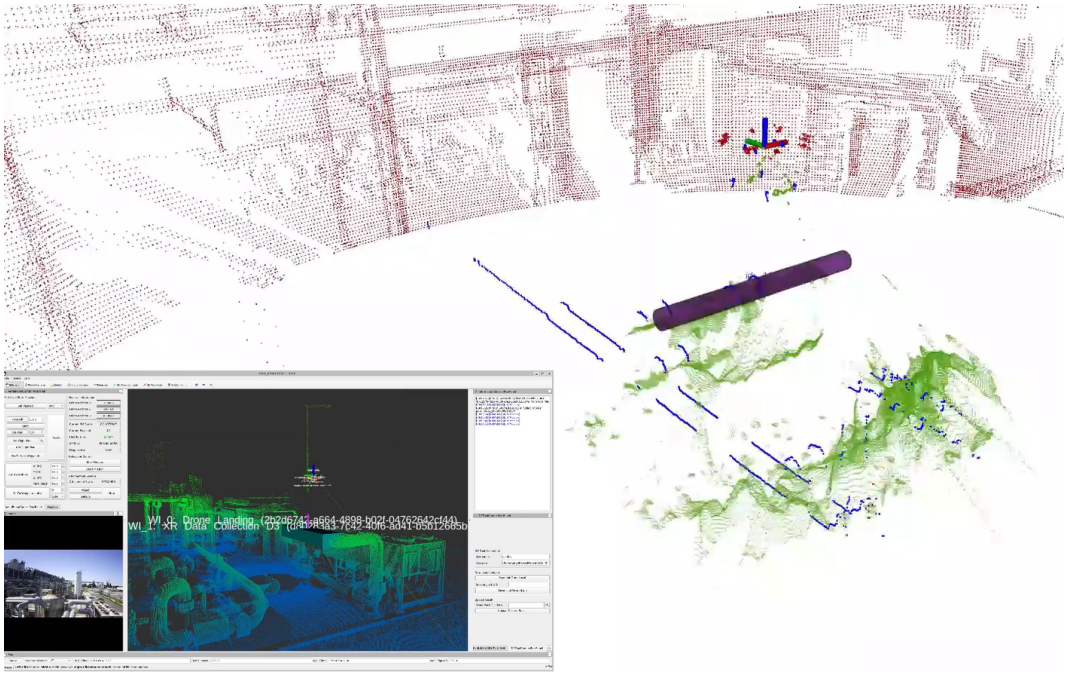

Fig. 19 Detection of pipe during final demonstration

On the other hand, the crawler detection algorithm perfectly identified and localized the XR crawler while performing the recovery mission. The image in Fig.20 shows the flight profile of a XR recovery mission. The top graph shows the attachment status (yellow) and the z_{status} and z_{ref}. On the graph below, it is possible to see the position status $(x, y)_{status}$ and reference $(x, y)_{ref}$. It is possible to see that once the UAV reached the position given by the crawler detector $(x, y)_{ref}$ started descending until it landed on top of the crawler, moment when the coupling mechanism activated in order to attach the crawler. Once this was completed the UAV took off, navigated to the home position and performed a landing operation.

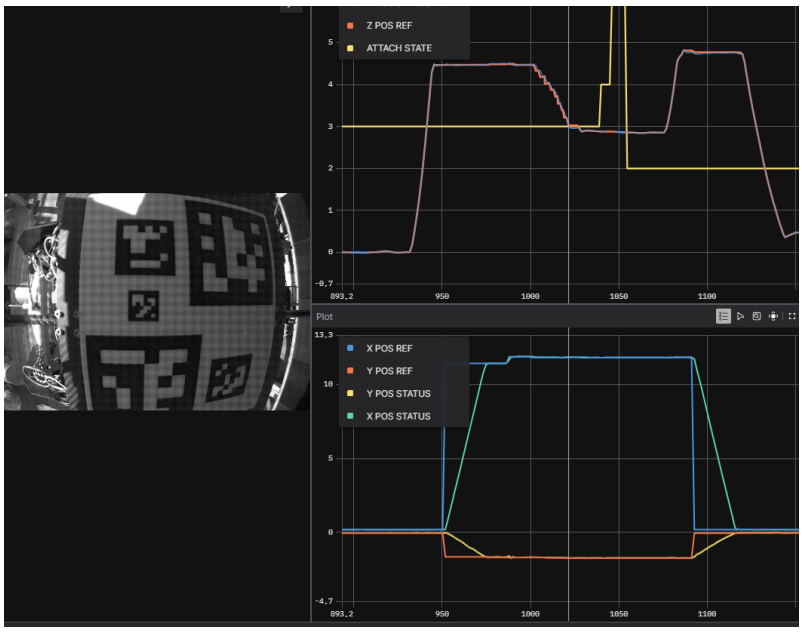

Fig. 20 ArUCO markers of XR crawler (left). Flight profile for recovery mission(right).

5 Conclusions

This paper has presented the design, autonomous stack and the validation of an autonomous aerial robotic system specifically designed for CUI inspections. This work pushes the previous work towards a mature and well tested concept, successfully reaching TRL7 through the demonstration in the real facilities.

This work has validated the complete autonomous workflow for deploying and recovering a robotic crawler in a complex and cluttered environment without GNSS for navigation. The final validations demonstrated the real value of this system compared to traditional methods for CUI inspections. A process that typically takes around 176 labor hours, the presented system could perform the same task in less than 4 hours, reducing the time by a factor of 44. Additionally, this system eliminates 100% the need for human exposure to work at height. A demonstration video of the SIMAR system showing these capabilities is available at `https://simar-project.eu/multimedia/#videos`

As a project, SIMAR presented the future of industrial inspections, where robotics is transforming the sector by eliminating the exposure of humans to unnecessary risks and making inspections safer, smarter and more efficient.

Acknowledgments

This work has received funding from the European Union's Horizon Europe research and innovation programme under grant agreement No. 101070604 (SIMAR project). The authors acknowledge the contributions of their colleagues to this work. In particular, Jesús Olmedo Pradas, David Tejero Ruiz, and Marco Montes Grova provided valuable technical input. Additional contributions from Roberto de Quero and his team are also recognized.

The support of other colleagues at CATEC during the development and testing phases is also acknowledged. Finally, the authors thank all partners within the SIMAR consortium for their collaboration and technical cooperation.

Declaration of Use of Artificial Intelligence

Artificial intelligence tools were used only for limited, acceptable purposes in accordance with the AI policy. Specifically, chat-based tools as chat-GPT were used to assist with language proofreading and minor text clarifications to improve readability and grammar. All scientific content, ideas, analyses, and conclusions were developed entirely by the authors and other contributors involved in SIMAR project.

References

[1] J. Nikolic, Michael Burri, J. Rehder, Stefan Leutenegger, C. Huerzeler, and Roland Siegwart. A uav system for inspection of industrial facilities. pages 1–8, 03 2013. ISBN: 978-1-4673-1812-9. doi: 10.1109/AERO.2013.6496959.

[2] Saeid Asadzadeh, Wilson Oliveira, and Carlos Souza Filho. Uav-based remote sensing for the petroleum industry and environmental monitoring: State-of-the-art and perspectives. *Journal of Petroleum Science and Engineering*, 208:109633, 10 2021. doi: 10.1016/j.petrol.2021.109633.

[3] Lutz Bretschneider, Sven Bollmann, Deborah Houssin-Agbomson, Jacob Shaw, Neil Howes, Linh Nguyen, Rod Robinson, Jonathan Helmore, Michael Lichtenstern, Javis Nwaboh, Andrea Pogány, Volker Ebert, and Astrid Lampert. Concepts for drone based pipeline leak detection. *Frontiers in Robotics and AI*, 11, 08 2024. doi: 10.3389/frobt.2024.1426206.

[4] Taha Enes Kon. The importance of the use of unmanned aerial vehicles (uavs) in the oil and gas industry. *Petroleum Science and Engineering*, 8:63–69, 07 2024. doi: 10.11648/j.pse.20240802.11.

[5] Fadl Abdellatif, Ali Alrasheed, Amjad Felemban, Ahmed Brahim, Hesham Jifri, Mohamed Abdelkader, Shehab Ahmed, and Jeff Shamma. Falconscan: A hybrid uav-crawler system for ndt inspection of elevated pipes in industrial plants. *Mechatronics*, 103:103239, 11 2024. doi: 10.1016/j.mechatronics.2024.103239.

[6] Miguel Trujillo, J. Ramiro Martinez-de Dios, Carlos Martín, Antidio Viguria, and Anibal Ollero. Novel aerial manipulator for accurate and robust industrial ndt contact inspection: A new tool for the oil and gas inspection industry. *Sensors*, 19:1305, 03 2019. doi: 10.3390/s19061305.

[7] Juan Carlos Trujillo, Rodrigo Munguia, Edmundo Guerra, and Antoni Grau. Cooperative monocular-based slam for multi-uav systems in gps-denied environments. *Sensors*, 18:1351, 04 2018. doi: 10.3390/s18051351.

[8] Marco A. Montes-Grova, Jaime Ortuño-Conde, David Tejero-Ruiz, Jesús Olmedo-Pradas, Francisco J. Pérez-Gran, Miguel A. Trujillo-Soto, and Antidio Viguria. Petrochemical industry aerial robotic inspection: A novel concept for landing and deploying robots on pipes. June 2024. doi: 10.1109/ICUAS60882.2024.10556863.

[9] Zhao Sz, Fei Kang, Junjie Li, and Chuanbo Ma. Structural health monitoring and inspection of dams based on uav photogrammetry with image 3d reconstruction. *Automation in Construction*, 130:103832, 10 2021. doi: 10.1016/j.autcon.2021.103832.

[10] Y. Boffill, I. Lombillo, H. Blanco, et al. Dronix: Inspección automatizada de infraestructuras mediante drones. In *REHABEND 2024 – Construction Pathology, Rehabilitation Technology and Heritage Management*, pages 579–588, 2024.

[11] Stefan Ivić, Bojan Crnković, Luka Grbčić, and Lea Matlekovic. Multi-uav trajectory planning for 3d visual inspection of complex structures, 04 2022. doi: 10.48550/arXiv.2204.10070.

[12] Voliro AG. Revolutionizing the future of contact-based aerial inspections with the voliro t version 5. Technical article / Application note, 2024.

[13] Roberto Giacchetta, Jose Brizuela, Jorge Cruza, and Francisco Alarcon. Hyfliers: drones inteligentes para automatizar la inspección por ultrasonido de infraestructuras de petróleo y gas. 06 2019.

[14] Y. Zhang, X. Li, J. Wang, et al. Falconscan: A hybrid uav–crawler system for ndt inspection of elevated pipes. *Expert Systems with Applications*, 2024.

[15] HyeongRyeol Kam, Sung-Ho Lee, Taejung Park, and Chang-Hun Kim. Rviz: a toolkit for real domain data visualization. *Telecommunication Systems*, 60:1–9, 10 2015. doi: 10.1007/s11235-015-0034-5.

[16] Fernando Caballero and Luis Merino. Dll: Direct lidar localization. a map-based localization approach for aerial robots. In *2021 IEEE/RSJ International Conference on Intelligent Robots and Systems (IROS)*, pages 5491–5498, 2021. doi: 10.1109/IROS51168.2021.9636501.

[17] Tixiao Shan, Brendan Englot, Drew Meyers, Wei Wang, Carlo Ratti, and Rus Daniela. Lio-sam: Tightly-coupled lidar inertial odometry via smoothing and mapping. In *IEEE/RSJ International Conference on Intelligent Robots and Systems (IROS)*, pages 5135–5142. IEEE, 2020.

[18] Francisco Romero-Ramirez, Rafael Muñoz-Salinas, and Rafael Medina-Carnicer. Speeded up detection of squared fiducial markers. *Image and Vision Computing*, 76, 06 2018. doi: 10.1016/j.imavis.2018.05.004.

[19] Sergio Garrido-Jurado, Rafael Muñoz-Salinas, Francisco Madrid-Cuevas, and Rafael Medina-Carnicer. Generation of fiducial marker dictionaries using mixed integer linear programming. *Pattern Recognition*, 51, 10 2015. doi: 10.1016/j.patcog.2015.09.023.

[20] David Tejero-Ruiz, Marco A. Montes-Grova, Francisco J. Pérez-Grau, Antidio Viguria, and Aníbal Ollero. Autonomous uav pipeline landing via depth-lidar fusion in gnss-denied refineries. *IEEE Robotics and Automation Letters*, 11(3):3692–3699, 2026. doi: 10.1109/LRA.2026.3662655.